Destabilization of epidemic models with the inclusion of realistic distributions of infectious periods

Alun L. Lloyd

Program in Theoretical Biology, Institute for Advanced Study, Einstein Drive, Princeton, NJ 08540, USA (*alun@alunlloyd.com*)

Most mathematical models used to understand the dynamical patterns seen in the incidence of childhood viral diseases, such as measles, employ a simple, but epidemiologically unrealistic, description of the infection and recovery process. The inclusion of more realistic descriptions of the recovery process is shown to cause a significant destabilization of the model. When there is seasonal variation in disease transmission this destabilization leads to the appearance of complex dynamical patterns with much lower levels of seasonality than previously predicted. More generally, this study illustrates how detailed dynamical properties of a model may depend in an important way on the assumptions made in the formulation of the model.

Keywords: epidemic model; infectious period distribution; seasonally forced dynamics

1. INTRODUCTION

Detailed studies of childhood viral disease incidence records have uncovered a wealth of fascinating dynamical patterns (London & Yorke 1973; Olsen & Schaffer 1990; Bolker & Grenfell 1993, 1995). Before the introduction of mass vaccination in the 1960s, measles incidence in large cities in the developed world exhibited recurrent epidemics. The most common of these patterns is the biennial cycle, with large outbreaks occurring every two years, but both annual and triennial behaviours are also seen (London & Yorke 1973; Bolker & Grenfell 1995). In many cases, the oscillations are less regular than those observed in other biological systems: although there is a definite multi-annual pattern, there can be considerable fluctuation in the sizes of the epidemics (Olsen & Schaffer 1990). Understanding the nature and origins of such epidemic behaviour has been of considerable interest to mathematical epidemiologists, as witnessed by the large literature in which the dynamics of epidemic models have been studied in great detail (Bartlett 1956; London & Yorke 1973; Dietz 1976; Grossman 1980; Schwartz & Smith 1983; Smith 1983a,b; Aron & Schwartz 1984; Schwartz 1985, 1992; Olsen & Schaffer 1990; Bolker & Grenfell 1993, 1995; Kuznetsov & Piccardi 1994; Engbert & Drepper 1994; Lloyd & May 1996; Keeling & Grenfell 1997; Earn *et al.* 2000).

The simplest models for childhood viral diseases exhibit damped oscillations towards an endemic equilibrium. These models, with the use of realistic parameter values, correctly predict that the damped oscillations occur on a time-scale of several years, but are unable to reproduce the recurrent epidemic pattern. Epidemiological studies (London & Yorke 1973; Fine & Clarkson 1982) reveal that the epidemic process is subject to considerable seasonal forcing; schools are major centres for the transmission of childhood diseases, and consequently transmission rates are much higher during school terms than during vacations. Seasonality can allow for the maintenance of recurrent epidemics within the model framework as it 'pumps' the damped intrinsic oscillations.

Low levels of seasonality lead to annual oscillations in incidence, but longer period oscillations can arise with stronger forcing (Dietz 1976; Smith 1983a,b; Aron & Schwartz 1984). More complex behaviours, such as deterministic chaos or intermittent behaviour can arise when the levels of seasonality are quite high (Olsen & Schaffer 1990; Engbert & Drepper 1994). These behaviours mimic many features of the incidence record, although it is not clear to what extent they provide a complete mechanistic explanation for them.

Most of the models employed in these studies of the dynamics of epidemics have employed a simple description of the disease process. One particular assumption made is that the time for which individuals remain infectious can be described by an exponential distribution. This distribution is biologically unrealistic, however, because it corresponds to the assumption that the chance of recovery in a given time interval is independent of the time since infection. This leads to the distribution of infectious periods being too dispersed. In reality, infectious periods are fairly closely centred about the mean duration of infection; the infectious period is unlikely to be either considerably shorter or considerably longer than the mean. Although non-exponential descriptions of the infectious period distribution have long been incorporated in models of long-lived infections, such as human immunodeficiency virus (HIV) (Blythe & Anderson 1988; Castillo-Chavez *et al.* 1989), it has commonly been believed that the description of the infectious period has little effect in models for short-lived infections (see, however, Grossman 1980; Lloyd 1996; Keeling & Grenfell 1997).

In this paper we consider the dynamical changes which result from the inclusion of non-exponential descriptions of the infectious period. After discussing modifications of the basic model which allow for the inclusion of such distributions, we discuss their effects on both unforced and seasonally forced models. In the unforced case, we use analytical and numerical techniques to generalize the work of Grossman (1980) and demonstrate that such distributions lead to destabilization of the endemic

equilibrium, with an increased time for damping of the intrinsic oscillations. In the forced case, we use numerical bifurcation analysis techniques to demonstrate that lower levels of seasonality are required to achieve biennial cycles in the more realistic model. Similarly, more complex dynamics can be achieved with much weaker forcing in more realistic models than in the basic model.

2. THE MODEL

In the standard susceptible, infected, recovered (SIR) model (see, for instance, Anderson & May (1991), for a full discussion of the model), the term describing the recovery of infective individuals is simply given by the product of the number of infectives, written as I, and the per-capita recovery rate, written as γ. This corresponds to assuming that the infectious periods are exponentially distributed, with mean duration of infection D equal to $1/\gamma$.

The general infectious period distribution is described by its probability density function, $f(\tau)$, which gives the probability of an individual infected τ time-units ago recovering in the time interval $(\tau, \tau + d\tau)$ as $f(\tau)d\tau$. This density function can be integrated to give the survivorship function,

$$F^s(y) = \int_y^\infty f(\tau)d\tau,\qquad(1)$$

which gives the probability that an individual remains in the infectious class for at least y time-units, given that they have not first died. Notice that the survivorship function is unity minus the cumulative density function corresponding to $f(\tau)$. Throughout what follows, to enable comparison between models which differ in their distributions of infectious periods, the mean duration of infection D will always be taken to be $1/\gamma$.

The inclusion of non-exponential distributions means that the chance of recovery depends on the time since infection, and hence the model needs to keep track of this information. Although this can be achieved in several ways, in this study we shall focus on a particularly simple formulation, involving the method of stages (Cox & Miller 1965; Anderson & Watson 1980; Lloyd 1996) because the resulting model is more amenable to analysis and numerical simulation. Alternative formulations include an integro-differential equation (IDE) formulation (Hethcote & Tudor 1980; Keeling & Grenfell 1997) or a partial differential equation (PDE) formulation (as employed in age-structured models; see, for instance, Anderson & May 1991). Further details can be found in electronic Appendix A available on The Royal Society's Web site.

Using the method of stages, the single infective class of the basic model is replaced by a series of n classes, or stages, arranged in series. Newly infected individuals enter the first stage before passing through each successive stage, with recovery corresponding to leaving the nth stage. If the time spent in each stage is assumed to be exponentially distributed, and the numbers of infectives in each stage are written I_j, then the rate at which infectives pass from the jth to the $(j + 1)$st stage is simply proportional to I_j. The total time spent in the n classes is

given by the sum of n independent exponential distributions. If the average waiting time in each stage is identical, this leads to a gamma distribution of infectious periods, the density function of which can be written

$$f(\tau) = \frac{(\gamma n)^n}{\Gamma(n)}\tau^{n-1}e^{-\gamma n\tau},\qquad(2)$$

Here, $\Gamma(n)$ is the gamma function. The variance of this distribution is $1/(n\gamma^2)$. Notice that both the exponential and delta (fixed duration) distributions are special cases of the gamma distribution, corresponding to $n = 1$ and $n \to \infty$, and that the gamma distribution is close to a normal distribution for large n. The probability density function of the gamma distribution is shown in figure 1a for $n = 1$, $n = 5$ and $n = 50$ stages.

Use of the stage approach leads to the following modified version of the SIR model:

$$\begin{aligned}
dS/dt &= \mu\mathcal{N} - \mu S - \beta SI,\\
dI_1/dt &= \beta SI - (n\gamma I_1 + \mu),\\
dI_2/dt &= n\gamma I_1 - (n\gamma I_2 + \mu),\\
&\vdots\\
dI_n/dt &= n\gamma I_{n-1} - (n\gamma I_n + \mu).
\end{aligned}\qquad(3)$$

Here it is assumed that the disease is non-fatal and confers permanent immunity upon recovery. S represents the number of susceptible individuals, I the total number of infectives, $I = \sum_{j=1}^n I_j$, and $\mathcal{N}$ the total population size. The birth and death rates are taken to be equal, and written as μ, leading to the total population size being constant. Because the size of the population is constant, the number of recovered individuals is given by $R = \mathcal{N} - S - I$. We assume that the infection term can be described by a mass-action term, with the transmission parameter written as β. Notice that a situation in which an individual's infectiousness varies over the course of an infection can easily be modelled by making the infection term a weighted sum over the I_j.

To model the effects of seasonal forcing, the β parameter is allowed to vary over the course of a year. Various functional forms have been suggested for this annual oscillatory term, ranging from simple phenomenological forms through to detailed functions which accurately model the opening and closing of schools across the year (Dietz 1976; Schenzle 1984). We choose to employ the simplest forcing term, namely the sinusoidal function

$$\beta(t) = \beta_0(1 + \beta_1\cos 2\pi t),\qquad(4)$$

where β_0 is the baseline transmission parameter and β_1 measures the strength of seasonality. Although less realistic than many functional forms, this remains the term most widely used in studies of the dynamics of SIR-type models, and so its use facilitates comparison of our results with those of other modelling studies.

3. RESULTS

(a) *Unforced model*

The dynamics of the unforced model are straightforward and are determined by the basic reproductive number, R_0, defined as the average number of secondary
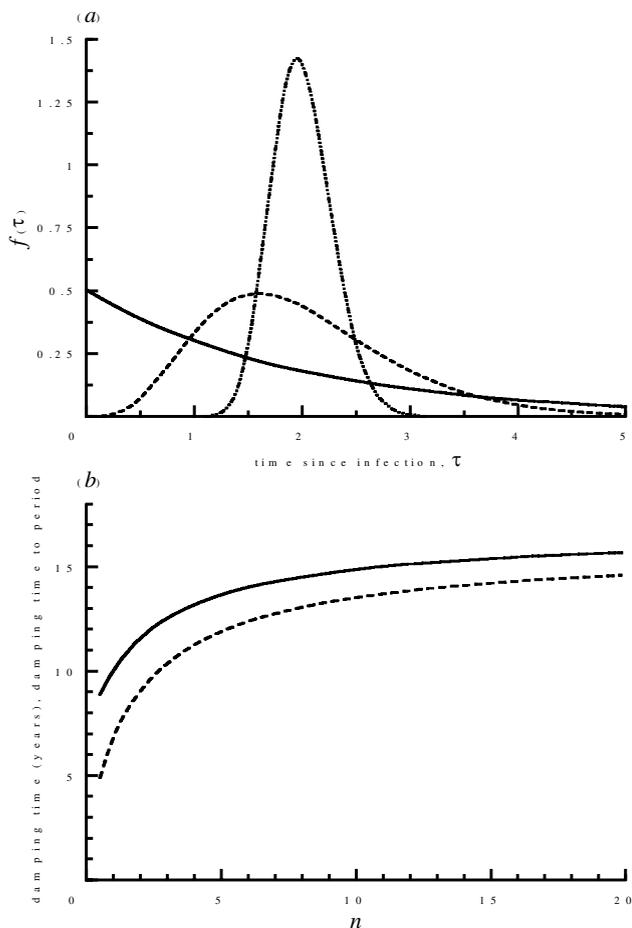
Figure 1. (*a*) Probability density function for the gamma distribution with $n = 1$ (exponential), $n = 5$ and $n = 50$ stages (solid, dashed and dot-dashed curves, respectively). (*b*) Damping time (solid curve) and ratio of damping time to period (dashed curve) for the damped oscillations in the unforced SIR model with a gamma distribution of infectious periods. Parameter values in the model are $\mathcal{N} = 10^7$ individuals, $\beta = 1000/\mathcal{N}$ individual^{-1} yr^{-1}, $\gamma = 100$ yr^{-1} and $\mu = 1/50$ yr^{-1}.

infections produced by a single infective individual in an entirely susceptible population (Macdonald 1952; Anderson & May 1991). R_0 is given by

$$R_0 = \frac{\beta \mathcal{N}}{\mu} \int_0^\infty (1 - e^{-\mu\tau}) f(\tau)\, d\tau, \tag{5}$$

which is the product of the rate at which new infections arise when a single infective is introduced into an entirely susceptible population and the average duration of infectiousness, corrected for mortality (Blythe & Anderson 1988). This expression can be rewritten in terms of the survivorship function (Hethcote & Tudor 1980; Castillo-Chavez *et al.* 1989)

$$R_0 = \beta \mathcal{N} \int_0^\infty F^s(\tau) e^{-\mu\tau} d\tau. \tag{6}$$

If R_0 is less than unity, the infection dies out; the disease-free equilibrium, for which $S^* = \mathcal{N}$ and $I^* = 0$, is globally stable (Hethcote & Tudor 1980). If R_0 is greater than unity, the disease-free equilibrium is unstable whilst the endemic equilibrium, for which $S^* = \mathcal{N}/R_0$ and $I^* = \mu(R_0 - 1)/\beta$,
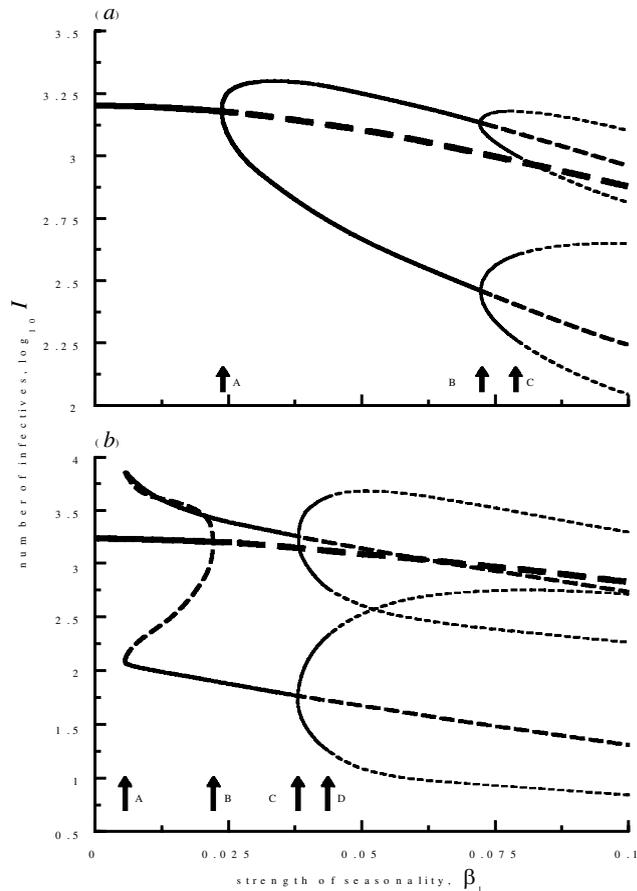

Figure 2. Parametric portraits for the seasonally forced basic SIR model ($n = 1$), showing the number of infectives at yearly intervals (times $t = 0, 1, 2, \ldots$) for various strengths of seasonality, β_1. Solid curves denote stable solutions, dashed curves unstable solutions. The heaviest lines denote annual oscillations, the medium curves represent biennial cycles and the faintest curves denote four-yearly cycles. (*a*) $\beta_0 = 500/\mathcal{N}$. A simple period doubling cascade is observed, as described in § 3(b). (*b*) $\beta_0 = 750/\mathcal{N}$. A more complex bifurcation sequence is observed, with the appearance of biennial cycles by a tangent bifurcation. Notice the coexistence of stable annual and biennial cycles between points A and B. The period two solution undergoes a period doubling bifurcation at point C, giving rise to a stable four-yearly cycle, which itself undergoes a period doubling bifurcation at D. Other parameter values are $\mathcal{N} = 10^7$ individuals, $\gamma = 100$ yr^{-1} and $\mu = 1/50$ yr^{-1}.

is locally asymptotically stable (Hethcote & Tudor 1980) and is believed to be globally stable.

As the mean duration of infection is short compared to the average life span ($\mu D \ll 1$), expression (5) for R_0 can be expanded as a series (Lloyd 1996), which, to first order, gives

$$R_0 = \beta \mathcal{N} D \left(1 - \frac{\mu D}{2}\{\sigma^2/D^2 + 1\}\right). \tag{7}$$

Here, σ^2 is the variance of the distribution of infectious periods. We notice that since the correction due to mortality is small, the expression for R_0 (and hence the equilibrium values of S and I) does not depend much on how infectious periods are distributed about their mean.
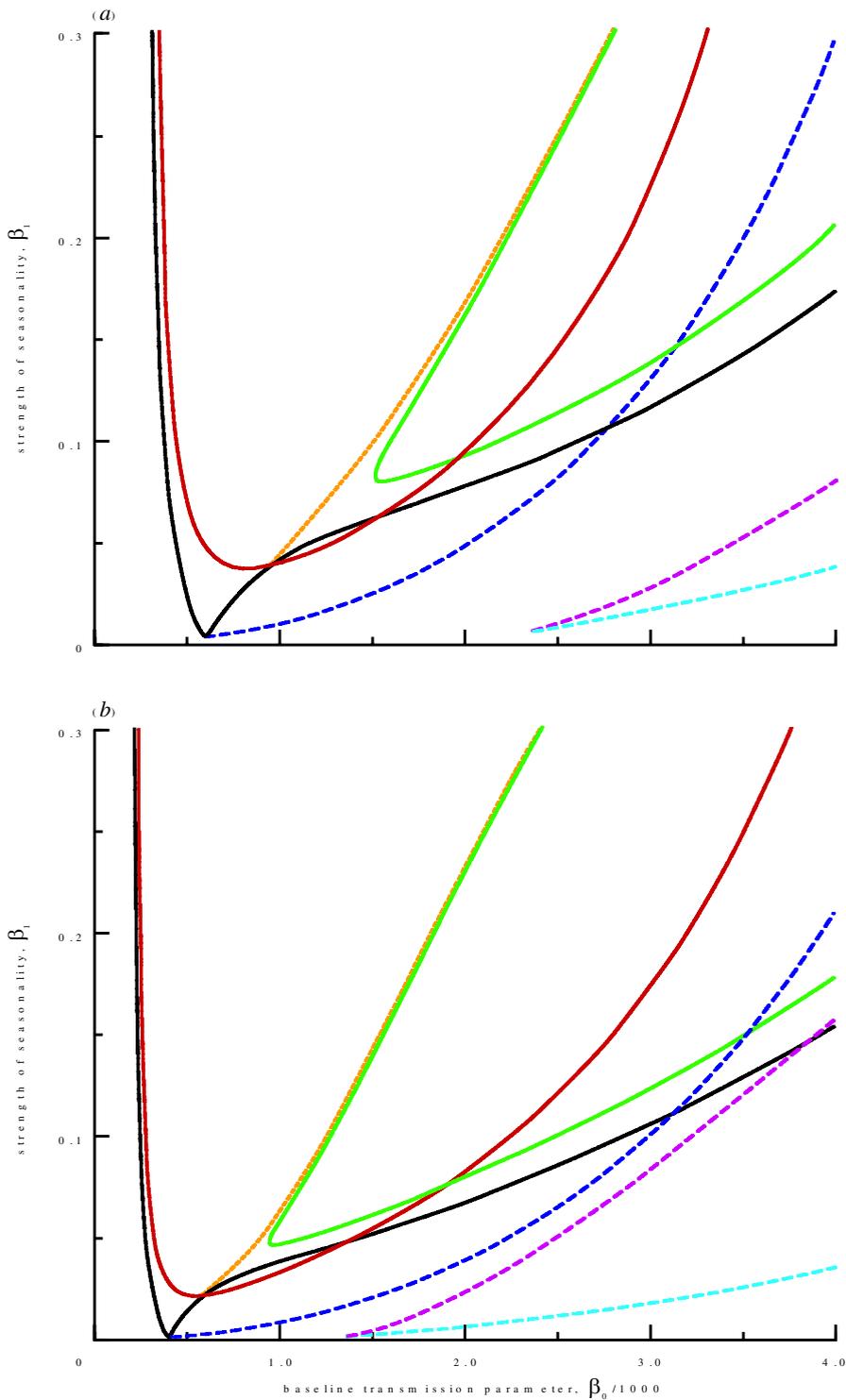
Figure 3. Bifurcation diagram for the seasonally forced SIR model. (*a*) Basic model, $n = 1$. (*b*) More realistic model, $n = 5$. Solid lines represent period doubling (flip) bifurcations, dashed lines represent tangent (saddle-node) bifurcations. The black curve traces out the parameter values at which period doubling of the annual cycle occurs. The dashed blue curve, which meets the black curve at its minimum, denotes the set of parameter values at which a tangent bifurcation creates a pair of biennial cycles. These two bifurcations are discussed at greater length in §3(b). Other bifurcations can occur involving annual or biennial cycles. The orange dashed curve denotes another set of tangent bifurcations which can occur involving biennial cycles. (This curve and the blue dashed curve have a common end-point at a value of (β_0, β_1) outside the region shown on this diagram.) The red and green curves denote period doubling bifurcations of biennial cycles, which involve four-yearly cycles. Finally, the cyan and magenta dashed curves are two sets of tangent bifurcations which create (and destroy) pairs of annual cycles. Other parameter values are as in figure 2.

The approach to the equilibrium can be described by linearizing the model, substituting $S(t) = S^* + s(t)$ and $I = I^* + k(t)$ and giving the small perturbations time dependence $\exp(\Lambda t)$. This leads to an equation which determines the values of Λ. The value of Λ which describes the approach to the equilibrium is obtained as the dominant root (i.e. the one with largest real part) of

$$\Lambda + \mu + \beta I^* - \beta S^*\{1 - G(\Lambda + \mu)\} = 0 \qquad (8)$$

(Hethcote & Tudor 1980; Lloyd 1996), where

$$G(\Lambda + \mu) = \int_0^\infty f(\tau)\mathrm{e}^{-(\Lambda+\mu)\tau}\mathrm{d}\tau. \qquad (9)$$

In the case of the gamma distribution, it is easy to see that

$$G(\Lambda + \mu) = \{1 + (\Lambda + \mu)/(n\gamma)\}^{-n}. \qquad (10)$$

Special cases of expression (10) are the exponential case ($n = 1$), for which $G(\Lambda + \mu) = \gamma/(\Lambda + \mu + \gamma)$, and the delta case ($n \to \infty$), for which $G(\Lambda + \mu) = \exp\{-(\Lambda + \mu)/\gamma\}$. In the former case, expression (8) determining stability reduces to the familiar expression which describes the stability of the endemic equilibrium of the standard SIR model (Anderson & May 1991). In this case, it is well known that the damping time is approximately $2A$ and that the period of oscillation is approximately $2\pi(AD)^{1/2}$, where A is the mean age at infection (which is approximately equal to L/R_0) and D is the mean duration of infection. In the delta case, the expression determining stability reduces to

$$(\Lambda + \mu) + \beta I^* - \beta S^*\mathrm{e}^{-(\Lambda+\mu)/\gamma} = 0, \qquad (11)$$

as obtained by Grossman (1980) (although notice that there is a typographical error in his equation 2.6b).

The stability result of Hethcote & Tudor (1980) shows that Λ has negative real part, and numerically it is found that, at least for realistic parameter values, Λ is complex. The equilibrium, therefore, is approached via damped oscillations. Figure 1*b* shows the damping time and ratio of the damping time to the period of the oscillations. Both properties of the oscillations, in marked contrast to R_0, do vary considerably as the parameter n of the gamma distribution is varied. In particular, in a generalization of the previously observed result for a fixed duration of infection (Grossman 1980), the damping time increases as n increases; the endemic equilibrium is less stable for less dispersed (i.e. more realistic) distributions of the infectious period.

More realistic distributions destabilize the endemic equilibrium, although not enough to lead to more complex dynamical behaviour. Such destabilization has important consequences for persistence properties of stochastic variants of the SIR model (Lloyd 2001*a*). Because, as is well known, stochastic effects can exert a larger effect on less stable systems, we would expect to see an increase in the chance of extinction with the inclusion of more realistic distributions in stochastic models. This has been observed numerically and is explored in more detail using analytical approaches elsewhere (Lloyd 1996, 2001*a*; Andersson & Britton 1997, 2000).

(b) *Forced model*

With the inclusion of seasonality, the endemic equilibrium loses its stability. When the forcing amplitude is small, the system undergoes annual oscillations about the endemic equilibrium, but as the strength of seasonality is increased a wide range of dynamic behaviours can be observed (Dietz 1976). Multiple attractor behaviour, when more than one long-term behaviour is possible for a given set of parameters, is commonly seen (Grossman 1980; Smith 1983*a*,*b*; Schwartz 1985). In such cases, the behaviour of the model depends not only on its parameter values, but also on the initial numbers of susceptibles and infectives. Set against this complex background, the notion of 'stability' is somewhat difficult to assess. One possible measure, which we shall employ here, is the ease with which seasonality can give rise to a particular dynamical behaviour, for instance biennial cycles.

To gain as much understanding of model behaviour as is possible, we focus on the qualitative behaviour of the system (asking, for instance, what types of periodic orbits are seen for a given set of parameters) and use bifurcation analysis to partition parameter space into regions within which the model behaves in a qualitatively similar fashion. Such a study can be performed using analytical (Grossman 1980; Schwartz & Smith 1983; Smith 1983*a*,*b*) or simulation-based (Bolker & Grenfell 1993; Engbert & Drepper 1994) techniques, but both of these methods have their drawbacks. We employ another approach, involving the numerical implementation of the analytical techniques used to study bifurcations, which more readily gives a global picture of the bifurcation structure in parameter space (see, for example, Kuznetsov 1995). Such techniques have been implemented in available software packages, such as CONTENT (Kuznetsov & Levitin 1995–1997), which we used to perform bifurcation analyses, following closely the methodology of Kuznetsov & Piccardi (1994). We emphasize that, whilst bifurcation analysis provides a detailed study of the dynamics of a model, these details are of less interest to us than the overall picture of what types of behaviour (e.g. biennial cycles, or more complex behaviours) are possible.

The simplest way of summarizing the changing dynamical patterns which result from altering a single parameter, in our case the strength of seasonality, is the parametric portrait (Kuznetsov & Piccardi 1994). Because the dynamics which result from annual forcing are of a multi-annual nature, in figure 2 we plot the numbers of infectives seen at times $t = 0, 1, 2, 3, \ldots$ (the iterates of the so-called time-one map) for each different value of β_1. An annual cycle corresponds to the appearance of a single point for a given value of β_1, a biennial cycle to the appearance of two points, and so on. Bifurcations can be seen to occur when the number of points, or their corresponding stability properties, change at some value of β_1.

Figure 2*a* illustrates the well-known period doubling scenario (Schwartz & Smith 1983; Aron & Schwartz 1984), in which the annual cycle loses stability as a stable biennial cycle appears (at the point labelled A). Further period doublings then occur (the first two at points B and C), eventually leading to the appearance of deterministic chaotic behaviour. Figure 2*b* shows that period doubling is not the only method by which biennial cycles can
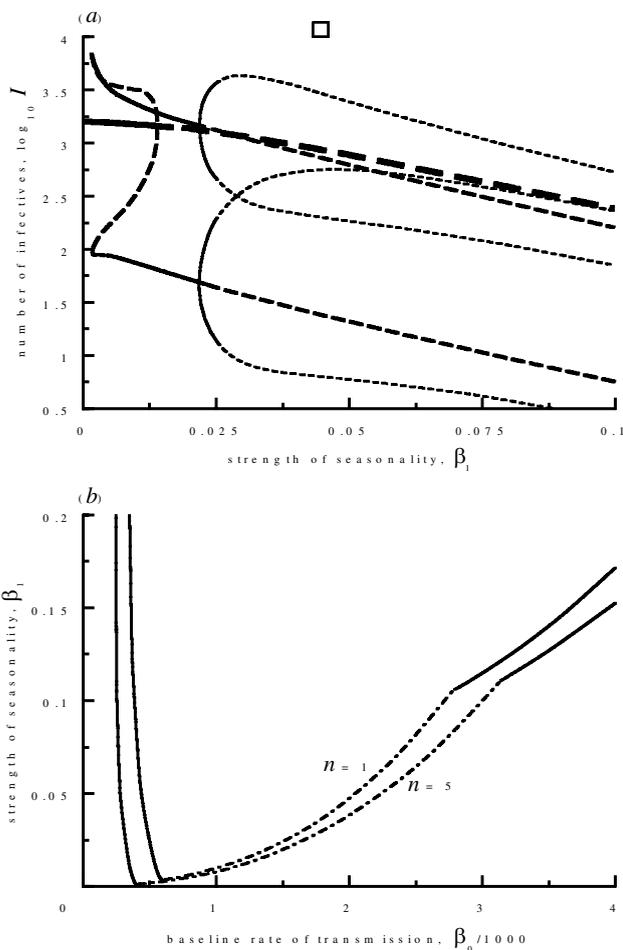
Figure 4. (*a*) Parametric portrait of the more realistic model, with $n = 5$ stages, when $\beta_0 = 500/N$, corresponding to the parametric portrait of the basic model shown in figure 2*a*. All parameter values and other details are as for figure 2*a*. Notice that the appearance of biennial cycles occurs for much weaker levels of seasonality, and occurs by a tangent bifurcation. (*b*) The strength of seasonality required to generate biennial cycles in the basic ($n = 1$) and more realistic ($n = 5$) models, for a range of values for the baseline rate of transmission (or, rescaling the axis, R_0). We indicate parameter ranges for which the biennial cycles are first generated by the period doubling (solid curve) or tangent (broken curve) bifurcations.

appear: a pair of biennial cycles, one stable and one unstable, appear at point A in a tangent (or saddle-node) bifurcation (Schwartz & Smith 1983; Smith 1983*b*). Such solutions often have quite large amplitudes, with very low infective levels in the inter-epidemic troughs. Further changes occur with strengthening seasonality, most notably at point B where the unstable biennial cycle collides with the stable annual cycle, resulting in the loss of the biennial cycle and the destabilization of the annual cycle. Notice that this scenario exhibits multiple attractor behaviour, with both stable annual and stable biennial cycles coexisting for a range of β_1-values.

Figure 2 demonstrates that the observed dynamical changes depend not only on the strength of seasonality, but also on the baseline rate of transmission (see also Earn *et al.* 2000). A bifurcation diagram (Kuznetsov & Piccardi 1994), which traces out bifurcation points as two or more parameters are changed, is a convenient way of summarizing the changing dynamical behaviours exhib-

ited by the model. Figure 3 shows the dependence of bifurcations affecting annual and biennial cycles on β_0 and β_1. For instance, the solid black curve illustrates how the β_1-value at which the annual cycle undergoes the period doubling bifurcation depends on β_0 (and hence on R_0). The tangent bifurcation which gave rise to the biennial cycle in figure 2*b* can be seen as the dark blue dashed curve. Because the parametric portraits shown earlier illustrate the bifurcations seen for a particular value of β_0 as β_1 is varied, they can be viewed as vertical slices through this bifurcation diagram. For further details on the bifurcations seen here, such as the tangent bifurcation which gives rise to a pair of high-amplitude annual cycles (cyan dashed curve), see Kuznetsov & Piccardi (1994).

So far, all of these analyses have been carried out on the basic SIR model (with exponential infectious period), and as such is entirely familiar from the work of Kuznetsov & Piccardi (1994). This analysis can be repeated for an *n*-stage model, and comparison of the bifurcation diagrams illustrates the dynamical changes which arise as a consequence of non-exponential distributions. Because the number of equations in the model is equal to $n + 1$, numerical bifurcation analyses become more time consuming as *n* increases, particularly if partial derivatives of the system are also calculated numerically. For this reason, we restricted attention to small values of *n*, and results are only shown for the $n = 5$ case.

Changing *n*, whilst keeping β_0 fixed, leads to dramatic changes in the parametric portrait of the model. Figure 4*a* shows the parametric portrait for the more realistic model with the same set of parameters as for the basic model shown in figure 2*a*. For this value of β_0, biennial cycles first appear by a tangent bifurcation in the more realistic ($n = 5$) model, as opposed to the period doubling seen in the basic ($n = 1$) exponential model. Biennial behaviour appears with a much lower level of seasonality in the more realistic model. As in the unforced model, the inclusion of more realistic distributions of infectious periods leads to destabilization of the model. Furthermore, the biennial cycle in the more realistic model has a much larger amplitude than that seen in the basic model for this value of β_0, which has important consequences for persistence in stochastic formulations of the model; these will be discussed later (§ 4).

Although the bifurcation sequence differed dramatically between figures 2*a* and 4*a*, in which β_0 was kept fixed, we notice that the behaviour of the more realistic model in this case is not unfamiliar: the parametric portrait of the more realistic model closely resembles that of the basic model, but for a different baseline rate of transmission (figure 2*b*). This is borne out upon examination of the bifurcation diagram of the more realistic model (figure 3*b*), which shows that the bifurcation pattern seen for more realistic models is qualitatively very similar to that seen for the basic model, but that there are significant quantitative differences in the parameter values at which various changes occur. In particular, a significant destabilization is seen, with dynamical changes occuring at much weaker levels of seasonality.

As a particular example of this destabilization, we focus on the bifurcation that first leads to the appearance of biennial cycles. We have seen that this can happen by

one of two mechanisms: a simple period doubling bifurcation or a tangent bifurcation. Figure 4*b* compares the bifurcation curves in the (β_0, β_1) plane between the $n = 1$ and $n = 5$ models, and shows that the biennial cycle appears with lower levels of seasonality in the more realistic model than in the standard model. We remark that this pattern would not be revealed by simply comparing the period doubling curves, or the tangent bifurcation curves, separately.

This analysis can be extended to study the further bifurcations that occur, such as those which ultimately lead to chaos. The bifurcation diagrams produced for behaviours with higher period are more complex yet, and so are not shown here. But the important observation is that more complex dynamics arise with much lower levels of seasonality in the more realistic model.

4. DISCUSSION

The inclusion of more realistic distributions of infectious periods within SIR-type models leads to a destabilization of the model, with more complex dynamics occuring for weaker levels of seasonality in the more realistic model. An epidemiologically important extension of these models allows for a latent period between the acquisition of infection and the start of infectiousness. The standard SEIR model (see, for instance, Anderson & May (1991) or Bolker & Grenfell (1993)) allows for such an exposed class of individuals, modelling their latent period by an exponential distribution, with average duration $1/\sigma$. Because the SIR model is a limiting case of the SEIR model as the latent period tends to zero, the destabilization phenomena described above also occur in SEIR models with short latent periods. More generally, the inclusion of an exposed class complicates the question of the stability of the endemic equilibrium: for instance, the damping time need no longer be an increasing function of the number of infective stages. However, when general distributions of both infectious and exposed periods are considered, it still appears that the inclusion of epidemiologically realistic distributions leads to destabilization compared to the basic SEIR model. (Details of the inclusion of the exposed class within the modelling framework, together with an analysis of the endemic equilibrium and its stability properties can be found in electronic Appendix B) Furthermore, bifurcation studies of seasonally forced SEIR models suggest that the destabilization phenomena described above also occur in SEIR models, even when the latent period is relatively long (see electronic Appendix B).

The destabilization of the dynamics of the seasonally forced model answers one of the central criticisms directed towards those who advocate deterministic chaos as an explanation for the complex dynamical patterns seen in the incidence records of childhood viral diseases. Based on studies which reconstruct the seasonal variations in transmission from the historical incidence records (London & Yorke 1973; Fine & Clarkson 1982), it has been argued that the observed levels of seasonality are far lower than those required to generate complex dynamics in the basic seasonally forced SEIR model (Pool 1989). However, these levels may be strong enough to generate complex behaviour in models which include more realistic

descriptions of the infectious period. This does not, however, address the difficulty that such models have in reproducing the observed patterns of disease persistence. Chaotic dynamics often (but not always) involve large swings in disease incidence, often with the numbers of infectives falling to well below a single individual. In such situations, the disease will go extinct (a so-called 'endemic fade-out'). We have seen that the dynamical destabilization is often accompanied by an increase in the amplitude of oscillations, which will tend to increase the chance of fade-out as the number of infective individuals falls to lower levels between epidemics.

Building on an earlier study (May 1986), Earn *et al.* (2000) demonstrated that the effects of vaccination or a change in the birth rate of the population can be studied by simply altering the baseline transmission parameter. The bifurcation diagrams presented here, therefore, can be employed to assess the impact of vaccination programmes, or changes in demographic parameters. For instance, figures 3 and 4*b* show that there is a window of baseline transmission rates for which biennial behaviour will be seen; increasing β_0 above or below this window (the former corresponds to an increase in the birth rate, and the latter to a decrease the birth rate, or vaccination of the population) leads to the loss of biennial dynamics, with annual behaviour instead being observed. (It should be borne in mind that this study has only examined annual and biennial behaviour, other multi-annual oscillations also being possible; see Earn *et al.* 2000.)

The similarity between the bifurcation diagrams of models with different distributions of infectious periods (figure 3*a,b*) opens up the possibility that the behaviour of the more realistic model, at least from the point of view of the qualitative dynamics of the deterministic system, could be captured by the simpler model, provided that an appropriate transformation of the parameters β_0 and β_1 is made. This observation echoes one made by Earn *et al.* (2000), who noted that the sequence of dynamical changes seen in an SEIR model with a realistic term-based forcing function was the same as that seen in an SEIR model with sinusoidal forcing, albeit one which employed a much lower amplitude of forcing. We remark that the converse implication of these results is important for the estimation of transmission parameters by fitting mathematical models to epidemiological data. As an example, because biennial patterns are obtained more easily in the more realistic SIR model discussed above, much lower levels of seasonality would be predicted if the more realistic model was fitted to a given epidemic time-series than if the basic model was used.

The appearance of multiple attractors and of higher amplitude oscillations in the deterministic model, both of which occur more easily in the more realistic model, have important consequences for the dynamics of stochastic formulations of the model. As has been frequently pointed out (Schwartz 1985; Engbert & Drepper 1994; Lloyd & May 1996; Earn *et al.* 2000), the coexistence of different attractors leads to the possibility of random effects playing an important dynamical role, as they can perturb the state of the system between different basins of attraction. In the deterministic system, many of these attractors exhibit large amplitude oscillations. They cannot correspond to attractors of the stochastic model,

because their minima fall well below a single infective individual. They can, however, be important for transient behaviour of the stochastic model, with realizations of the stochastic model shadowing trajectories of the deterministic system before undergoing fade-out.

Assumptions concerning the distribution of infectious periods affect not only endemic behaviour, but also the initial epidemic behaviour. Elsewhere (Lloyd 2001*b*), we show that for a disease with a given basic reproductive number, the rate of increase of the number of infectives during the epidemic phase depends heavily on the detailed properties of the disease process. Less dispersed distributions of infectious periods lead to more rapid growth of epidemics (Anderson & Watson 1980; Lloyd 1996), but more importantly, the inclusion of a latent period slows the epidemic, with less dispersed latent periods leading to greater reductions (Anderson & Watson 1980; Nowak *et al.* 1997). These observations have important implications for the estimation of the basic reproductive number from initial epidemic data, most importantly that neglecting latent periods can lead to severe underestimates of R_0. Because the critical vaccination fraction (Anderson & May 1991) is determined by R_0, such underestimates are a severe problem as they lead to over-optimistic estimates for the vaccination coverage required to achieve disease eradication.

The unforced SIR model is an instance of the predator–prey type models widely used in population biology, and as a consequence the results presented here may be important in other areas. As an example, the simplest models used to describe the interactions of viruses and the immune system in diseases such as HIV are of an almost identical form (see, for example, Nowak *et al.* 1997). Dynamical properties of such models will also be affected by assumptions of the type discussed here, and so the results concerning destabilization of the endemic equilibrium are of clear importance to studies which attempt to estimate population parameters by fitting mathematical models to virus load data obtained during the approach to the viral quasi-equilibrium which is established following initial infection (see, for instance, Stafford *et al.* 2000).

Because detailed studies of dynamical properties form a large part of many mathematical explorations of biological systems, the results of studies such as this have important wider implications. An important issue whenever a mathematical model is used to address a biological question is of model robustness: if we are to have confidence in our predictions, we need to be sure that the observed behaviour is not dependent on the detailed assumptions which underlie the model. This study has highlighted the point that model robustness depends on the question being asked of the model. Whilst the equilibrium levels of susceptibles and infectives were relatively insensitive to the assumed infectious period distribution, the dynamical properties of the model were quite sensitive to the assumed distribution. Detailed dynamical properties can be quite dependent on assumptions which are routinely made in the formulation of mathematical models for biological systems.

REFERENCES

Anderson, D. & Watson, R. 1980 On the spread of a disease with gamma distributed latent and infectious periods. *Biometrika* **67**, 191–198.

Anderson, R. M. & May, R. M. 1991 *Infectious diseases of humans: dynamics and control*. Oxford University Press.

Andersson, H. & Britton, T. 1997 *Fade-outs for SIR epidemics with demography and generalized infectious period*. Report 1997:28, Uppsala University Department of Mathematics, Sweden.

Andersson, H. & Britton, T. 2000 Stochastic epidemics in dynamic populations: quasi-stationarity and extinction. *J. Math. Biol.* **41**, 559–580.

Aron, J. L. & Schwartz, I. B. 1984 Seasonality and period-doubling bifurcations in an epidemic model. *J. Theor. Biol.* **110**, 665–679.

Bartlett, M. S. 1956 Deterministic and stochastic models for recurrent epidemics. In *Proceedings of the Third Berkeley Symposium on Mathematical Statistics and Probability* (ed. J. Neyman), pp. 81–109. Berkeley, CA: University of California Press.

Blythe, S. P. & Anderson, R. M. 1988 Distributed incubation and infectious periods in models of the transmission dynamics of the human immunodeficiency virus (HIV). *IMA J. Math. Appl. Med. Biol.* **5**, 1–19.

Bolker, B. M. & Grenfell, B. T. 1993 Chaos and biological complexity in measles dynamics. *Proc. R. Soc. Lond.* B **251**, 75–81.

Bolker, B. & Grenfell, B. 1995 Space, persistence and dynamics of measles epidemics. *Phil. Trans. R. Soc. Lond.* B **348**, 309–320.

Castillo-Chavez, C., Cooke, K., Huang, W. & Levin, S. A. 1989 On the role of long incubation periods in the dynamics of acquired immunodeficiency syndrome (AIDS). *J. Math. Biol.* **27**, 373–398.

Cox, D. R. & Miller, H. D. 1965 The theory of stochastic processes. London: Chapman & Hall.

Dietz, K. 1976 The incidence of infectious diseases under the influence of seasonal fluctuations. *Lect. Notes Biomath.* **11**, 1–5.

Earn, D. J. D., Rohani, P., Bolker, B. M. & Grenfell, B. T. 2000 A simple model for complex dynamical transitions in epidemics. *Science* **287**, 667–670.

Engbert, R. & Drepper, F. R. 1994 Chance and chaos in population biology—models of recurrent epidemics and food chain dynamics. *Chaos, Solitons & Fractals* **4**, 1147–1169.

Fine, P. E. M. & Clarkson, J. A. 1982 Measles in England and Wales. 1. An analysis of factors underlying seasonal patterns. *Int. J. Epidemiol.* **11**, 5–14.

Grossman, Z. 1980 Oscillatory phenomena in a model of infectious diseases. *Theor. Popul. Biol.* **18**, 204–243.

Hethcote, H. W. & Tudor, D. W. 1980 Integral equation models for endemic infectious diseases. *J. Math. Biol.* **9**, 37–47.

Keeling, M. J. & Grenfell, B. T. 1997 Disease extinction and community size: modeling the persistence of measles. *Science* **275**, 65–67.

Kuznetsov, Y. A. 1995 *Elements of applied bifurcation theory*. New York: Springer.

Kuznetsov, Y. A. & Levitin, V. V. 1995–1997 *CONTENT: a multi-platform environment for analyzing dynamical systems*. Dynamical Systems Laboratory, Centrum voor Wiskunde en Informatica, Amsterdam. Available at ftp.cwi.nl/pub/CONTENT.

Kuznetsov, Y. A. & Piccardi, C. 1994 Bifurcation analysis of periodic SEIR and SIR epidemic models. *J. Math. Biol.* **32**, 109–121.

Lloyd, A. L. 1996 The effects of more realistic distributions of infectious periods in epidemic models. In *Mathematical models for spatial heterogeneity in population dynamics and epidemiology*. DPhil. thesis, University of Oxford, UK.

Lloyd, A. L. 2001*a* Realistic distributions of infectious periods in epidemic models: changing patterns of persistence and dynamics. *Theor. Popul. Biol.* (Submitted.)

Lloyd, A. L. 2001*b* The dependence of viral parameter estimates on the assumed viral lifecycle: limitations of studies of viral load data. *Proc. R. Soc. Lond.* B **268**, 847–854.

Lloyd, A. L. & May, R. M. 1996 Spatial heterogeneity in epidemic models. *J. Theor. Biol.* **179**, 1–11.

London, W. P. & Yorke, J. A. 1973 Recurrent outbreaks of measles, chickenpox and mumps. I. Seasonal variation in contact rates. *Am. J. Epidemiol.* **98**, 453–468.

Macdonald, G. 1952 The analysis of equilibrium in malaria. *Trop. Dis. Bull.* **49**, 813–829.

May, R. M. 1986 Population biology of microparasitic infections. In *Mathematical ecology, biomathematics*, vol. 17 (ed. T. Hallam & S. Levin), pp. 405–442. New York: Springer.

Nowak, M. A. (and 10 others) 1997 Viral dynamics of primary viremia and antiretroviral therapy in simian immuno-deficiency virus infection. *J. Virol.* **71**, 7518–7525.

Olsen, L. F. & Schaffer, W. M. 1990 Chaos versus noisy periodicity: alternative hypotheses for childhood epidemics. *Science* **249**, 499–504.

Pool, R. 1989 Is it chaos, or is it just noise? *Science* **243**, 25–28.

Schenzle, D. 1984 An age-structured model of pre- and post-vaccination measles transmission. *IMA J. Math. Appl. Med. Biol.* **1**, 169–191.

Schwartz, I. B. 1985 Multiple stable recurrent outbreaks and predictability in seasonally forced nonlinear epidemic models. *J. Math. Biol.* **21**, 347–361.

Schwartz, I. B. 1992 Small amplitude, long period outbreaks in seasonally driven epidemics. *J. Math. Biol.* **30**, 473–491.

Schwartz, I. B. & Smith, H. L. 1983 Infinite subharmonic bifurcation in an SEIR epidemic model. *J. Math. Biol.* **18**, 233–253.

Smith, H. L. 1983*a* Subharmonic bifurcation in an *S-I-R* epidemic model. *J. Math. Biol.* **17**, 163–177.

Smith, H. L. 1983*b* Multiple stable subharmonics for a periodic epidemic model. *J. Math. Biol.* **17**, 179–190.

Stafford, M. A., Corey, L., Cao, Y., Daar, E. S., Ho., D. D. & Perelson, A. S. 2000 Modeling plasma viral concentration during primary HIV infection. *J. Theor. Biol.* **203**, 285–301.

Electronic appendices to this paper can be found at http://www.pubs.royalsoc.ac.uk.